Adsorption 5, 305–312 (1999)

Microstructural Analysis of the Effects of Poly(ethylene glycol) on an Acid Catalyzed Sol-Gel Derived Ceramic Material

P. ÅGREN
Department of Physical Chemistry, Åbo Akademi University, Porthaninkatu 3-5, FIN-20500 Turku, Finland

P. PENDLETON
School of Chemical Technology, University of South Australia, Mawson Lakes, South Australia 5095, Australia

J.B. ROSENHOLM
Department of Physical Chemistry, Åbo Akademi University, Porthaninkatu 3-5, FIN-20500 Turku, Finland

Received May 22, 1998; Revised September 22, 1998; Accepted October 12, 1998

Abstract. Ceramic materials have been derived from an acid catalyzed sol-gel process. The addition of different molecular weights and concentrations of polyethylene glycol (PEG) to the sol mixture modifies the phase behaviour of the sol-gel process. The resulting gel is burned at 973 K to make porous ceramic materials. Nitrogen adsorption-desorption isotherms are used to assess the effects of PEG on the internal structure of the burned ceramic material. These isotherms indicate an extensive pore network exists consisting of micropores and mesopores. In the micropore region of the isotherms, the α_S-plot analysis reveals changes in specific primary micropore volumes, specific total pore volumes, specific external surface areas and specific SPE surface area when PEG is added in the sol-gel process. The average pore width and the overall mesopore size distribution curves shift to higher pore size values and ranges on addition of PEG to the sol-gel mixture. The presence of PEG during the sol-gel process leads to an apparent narrowing of the micropore size distribution. The results of this work clearly indicate that the molecular weight and the concentration of a polymer, such as PEG, influences the eventual internal structure of a ceramic after burning.

Keywords: silica, synthesis techniques, characterisation of structure, pore condensation

Introduction

The synthesis of high specific surface area materials containing a controlled porosity is of great importance in the development of catalysts, catalyst supports and porous membranes used in synthesis and separation processes. The sol-gel route of producing amorphous silicon oxides has been studied extensively and reported widely (Brinker and Scherer, 1990). Silicon alkoxides, such as tetraethylorthosilicates (TEOS) as the silicon source, offers one of several methods of mixing gel-forming species on a molecular scale at relatively low temperatures. In the first reaction step, silanol forms by hydrolysis which, in the second reaction step, by condensation forms polysilicates. Generally, acid catalysed hydrolysis leads to polymeric sols, while base catalysed hydrolysis leads to particulate sols. To improve the nature of ceramic materials made by sol-gel synthesis, various, different additives are used. Their effects on the synthesis are not always clear. Cracking in the dried matrix is a serious problem when making ceramic materials, consequently, different drying control additives have been employed (Brinker and Scherer, 1990). Surfactants have been used as additives to reduce the interfacial energy of liquids contained in pores in an attempt to reduce capillary stresses

(Brinker and Scherer, 1990). Surfactants are also used as organic templates (creating surfactant-liquid-crystal structures) in the silicate condensation reaction forming ceramic materials such as MCM-41, exhibiting a regular pore structure (Beck et al., 1992). The effects of different types of water soluble additives on sols, gels and ceramic materials have been reported widely in the literature (Matsuoka et al., 1991; Julbe et al., 1994; Nakanishi et al., 1994; Nakanishi et al., 1992; Kunze and Segal, 1991). The present work focuses on how the pore structure of the ceramic material is affected by the addition of a water soluble polymer to the sol-gel reaction. Different concentrations of three different molecular weights of poly(ethylene glycol) are assessed. Studies on how the polymers affect the phase behaviour, gelation time and the rheological behaviour of the sols and gels have been reported elsewhere (Ågren and Rosenholm, 1998).

The principal characterisation of the ceramics reported here consists of nitrogen adsorption isotherms. The α_S-analysis comparison plot method has become widely accepted as a feasible method of porosity assessment. This methodology readily identifies the presence of micropores and mesopores; recently, the microporosity analysis has been extended to the identification of so-called primary and secondary micropore volumes. These volumes are held responsible for filling and condensation processes (Kaneko et al., 1992; Kaneko and Ishii, 1992; Kaneko, 1994; Hanzawa et al., 1996).

Experimental

Silica gels were prepared by the sol-gel method from a mixture of water ($R > 18$ MΩ cm), nitric acid (ex. Merck), tetraethylorthosilicate (TEOS) and poly(ethylene glycol) (PEG) (ex. Aldrich). PEG of different molecular weights 4,600 g/mol (ex. Aldrich), 10,000 g/mol (ex. Aldrich) and 35,000 g/mol (ex. Merck) and concentrations 0, 1, 5 and 9 wt% were dissolved in an aqueous acid solution with the aid of rapid stirring. The TEOS was subsequently added drop-wise, creating two phases. The reaction proceeds via hydrolysis assuring complete "solubilisation" by forming the hydrophilic silanol and ethanol, as a by-product, which acts as an interphase solvent. Stirring continued until the reaction was complete, noted via the steady-state temperature of the system. Although the molecular weight of the polymer was a variable, the molar ratios of water to nitric acid (57.8 : 1, based on 100 wt% HNO_3) and water to TEOS (14.7 : 1) were kept constant. Aliquots (5 ml) of the solutions were transferred to plastic test tubes and allowed to gel in a thermostated bath held at 313 K for different, known lengths of time. Both the concentration and the molecular weight of the polymer affect the gelation time. The gels were aged for 18 h, during which they form ingots similar in shape to their containers, and subsequently placed in parafilm-capped test-tubes and washed three times for periods of 6 h, 6 h and 12 h with 40 ml of 50 %vol/vol ethanol and once with 40 ml of 1 M HNO_3 for 24 h. Thereafter, the gels were washed twice in 40 ml of de-ionised water for ≈30 s each time, and finally with acetone for 30 s. During these washing periods, the unreacted reactants were expected to be completely leached from the final product. Small breathing holes were made in the parafilm lids prior to drying the gels at 313 K for 6 days in a ventilated oven. After drying, the ingots were placed in crucibles and sintered by heating at 10 K/h to 973 K then held at this temperature for 2 h. Subsequently, the heating was switched off and the oven allowed to cool to room temperature. This sintering process completely oxidised the organic polymer, producing a porous silica ceramic.

Nitrogen adsorption and desorption isotherms, leading to surface area and porosity evaluations, were measured using a Carlo Erba Instruments Sorptomatic 1900. Sample activation consisted of evacuating the sample in vacuo and heating to 573 K for 5 h, to remove any physically adsorbed materials. The non-porous hydroxylated silica Fransil I was used as a standard for subsequent silica gel isotherm analyses. In all cases, nitrogen adsorption-desorption isotherms were determined at 77 K.

Results and Discussion

The nomenclature used to describe the ceramic samples in this work is as follows: samples of PEG of $M_W =$ 4600 g/mol at concentrations of 1, 5 or 9%wt/wt during the sol-gel process have the codes PEG461, PEG465 or PEG469.

The nitrogen adsorption isotherms of the various ceramic samples prepared in this work are summarised in Figs. 1–3. The sample prepared in the absence of PEG, identified as PEG0 in Fig. 1, exhibits Type I character, indicating the presence of micropores only. All of the isotherms of the samples prepared in the presence of PEG (except PEG105) may be characterised as (approximately) Type IV with a type H4 hysteresis loop in

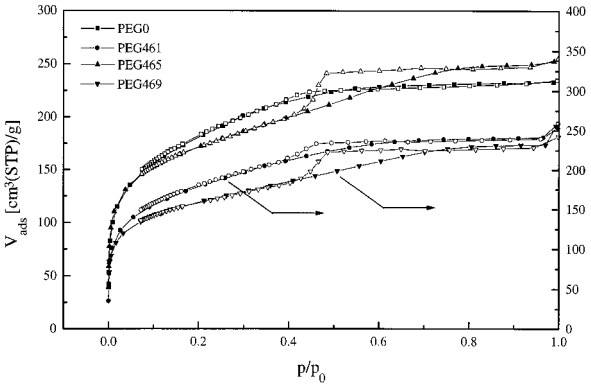

Figure 1. The N_2 adsorption-desorption isotherms at 77 K for samples PEG0, PEG461, PEG465 and PEG469. Solid symbols denote adsorption and open symbols denote desorption.

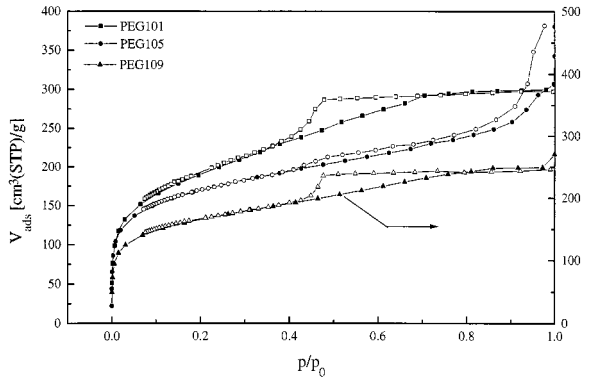

Figure 2. The N_2 adsorption-desorption isotherms at 77 K for samples PEG101, PEG105 and PEG109. Solid symbols denote adsorption and open symbols denote desorption.

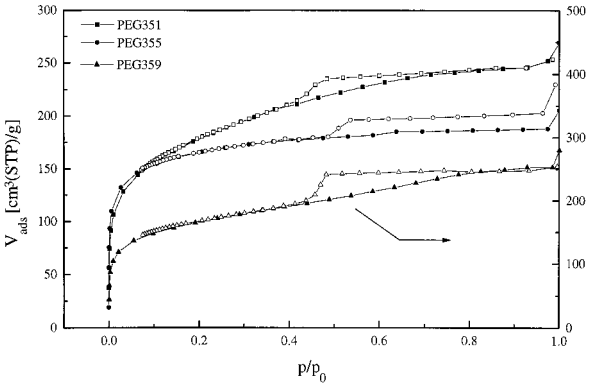

Figure 3. The N_2 adsorption-desorption isotherms at 77 K for samples PEG351, PEG355 and PEG359. Solid symbols denote adsorption and open symbols denote desorption.

the desorption process. Sample PEG105 exhibits a type H3 hysteresis loop. All of the samples had a marked adsorption uptake at pressures below $0.05p_0$, suggesting the presence of micropores, and thereafter, a monotonic increase in amount adsorbed until $\approx 0.8p_0$, above which the volume adsorbed was pressure independent. We attribute the linear rise in the amount adsorbed in the relative pressure range $0.1 < p/p_0 < 0.4$ to an overlap of condensation filling in the largest micropores and multilayer formation prior to lens formation and capillary condensation in the smaller mesopores. The rise in amount adsorbed in the range $0.4 < p/p_0 < 0.95$ is attributed to capillary condensation.

Figure 2 summarises the adsorption isotherms of the samples prepared using PEG with a $M_W =$ 10000 g/mol. Each of these samples exhibit Type IV adsorption characteristics; the hysteresis loops for both PEG101 and PEG109 are type H4 while that for PEG105 is type H3. The PEG105 isotherm clearly suggests a different pore structure and pore size distribution to the remaining materials reported herein. This difference is a consequence of a macrophase separation in the liquid mixture prior to the sol-gel transition. The phase behaviour of these mixtures is discussed elsewhere (Ågren and Rosenholm, 1998).

Figure 3 shows the adsorption isotherm for the silica ceramics prepared with PEG of $M_W = 35000$ g/mol. Each isotherm is Type IV, however, the isotherm of sample PEG355 shows a more distinct Type I character in the adsorption branch, suggesting a narrower micropore size distribution than any of the other samples produced in all of the silica syntheses. A macrophase separation was also observed prior to the sol-gel transition during the synthesis of the PEG351 and PEG355 samples. The influence of phase separation is not apparent from adsorption isotherms due to the similarity of the adsorption isotherms of these samples to those of all of the remaining silicas in this study.

α_S-Plot Analysis

In his recent porosity analysis review, Kaneko (1994) discussed the identification of filling and condensation regimes as distinct regions within an α_S-plot analysis, as originally suggested by Sing (1972, 1982). These analyses require precise, high resolution adsorption isotherm data, such as those provided in Figs. 1–3. High resolution α_S-analyses were made to define the specific micropore volume and external specific surface area of each sample, as well as identify the filling

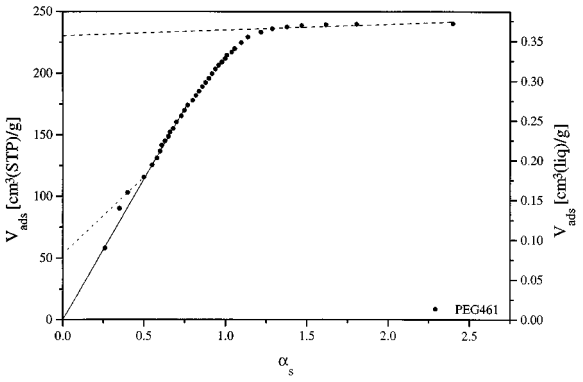

Figure 4. The α_S plot of sample PEG461.

and condensation regimes of the adsorption isotherms. The filling process is associated with primary micropores, typically of width <2–3σ, where σ is the nominal diameter of the adsorptive. In this case, the limit of primary micropores is ≈0.7–1.0 nm. The condensation process is attributed to an entropy-dominated adsorption occurring in secondary micropores of width ≈0.85 nm $< w <$ 2.0 nm.

The α_S-analysis of the sample PEG461, shown in Fig. 4, indicates two linear regions. The lower region prior to the upward swing, $0.4 < \alpha_S < 0.6$, is interpreted as primary micropore filling. The intersection of this linear slope with the ordinate axis gives the primary micropore volume as 0.083 cm^3(liq)/g. The linear region for $\alpha_S > 1.25$, is attributed to adsorption on the external surface area of the solid and possibly due to capillary condensation within the solid. The intersection of this linear slope is equivalent to the total pore volume of the material, 0.356 cm^3(liq)/g. The lack of a distinct secondary micropore regime blurs the correct allocation of volume to secondary micropores and mesopores. We suggest the 0.273 cm^3(liq)/g be attributed collectively to both pore sizes.

The shape of the adsorption isotherms in the relative pressure range $0 > p/p_0 > 0.5$ substantiates a more general interpretation of the pore volumes. The α_S-analysis for all of the samples prepared in the presence of PEG may be generalised as follows:

i) a linear region for $V_{ads} = f(\alpha_S)$ for $0.4 < \alpha_S < 0.6$,
ii) a step in the volume adsorbed at $\alpha_S = 0.6$, followed by,
iii) a second linear region for $V_{ads} = f(\alpha_S)$ for $0.6 < \alpha_S < 1.0$,
iv) a second step at $\alpha_S \approx 1.0$–1.2, followed by,
v) a region where V_{ads} is not directly proportional to α_S for $1.25 < \alpha_S < 2.5$.

These linear regions and steps are most clearly exemplified by the α_S-plot in Fig. 4. The primary and total pore volumes determined from the PEGxxx α_S-plots are summarised in Table 1. This allocation of pore volume leads to the question of properly defining each pore type on the adsorption isotherm. In each case, the transition from the region bounded by (iii) and (v) above, described as the step (iv) is visible in the α_S-plots. We attribute this step to a region where

Table 1. Values for specific primary micropore volume, specific total pore volume, specific secondary micropore + mesopore volume, specific external surface area and specific SPE surface area determined from the α_S plots, and additionally the specific BET surface area for all the prepared ceramic materials.

Sample	Molecular weight of PEG (g/mol)	Concentration of PEG (wt-%)	Specific primary μpore volume (ml/g)	Specific total pore volume (ml/g)	Specific secondary μpore + mesopore volume (ml/g)	Specific external surface area (m^2/g)	Specific BET surface area (m^2/g)	Specific SPE surface area (m^2/g)
PEG0	None	0	0.067	0.35	0.283	8.77	657	663
PEG461	4600	1	0.083	0.356	0.273	13.57	643	659
PEG465	4600	5	0.095	0.37	0.275	13.03	624	653
PEG469	4600	9	0.072	0.344	0.272	11.48	577	607
PEG101	10000	1	0.067	0.447	0.38	12.52	689	699
PEG105	10000	5	0.098	0.307	0.209	70.03	628	659
PEG109	10000	9	0.077	0.359	0.282	20.15	603	638
PEG351	35000	1	0.093	0.358	0.265	17.93	644	660
PEG355	35000	5	0.109	0.282	0.173	5.11	610	681
PEG359	35000	9	0.085	0.364	0.279	20.24	605	635

multi-layer adsorption occurs in the wider micropores, prior to adsorption condensation in any mesopores, as originally suggested by Kaneko and Ishii (1992). These authors suggested a method to calculate the specific, secondary pore external surface area (the specific SPE surface area) by an analysis of the linear region in section iii). In Fig. 4, the linear region passes through the origin (as the solid line) and is used to calculate the specific SPE surface area. The intercept of the dashed-line in region (v) is considered to be equivalent to the total pore volume; the slope of this line leads to the adsorbent's specific (external) surface area. Similar observations may be drawn for all the other samples (results not shown). The secondary micropore and mesopore volumes and the SPE surface area are also summarised in Table 1. In Table 1, clearly, the largest primary micropore volumes occur for samples containing 5% PEG however, the reason for this is not readily apparent.

Good agreement exists between PEG0 and the samples PEG46x for the specific total pore volumes. The reason for this is probably due to the presence of a single phase during the sol-gel processing. For the larger molecular weight templated samples of PEG-synthesised silicas, the macrophase separation at 5 wt% PEG may be an explanation for the lower specific total pore volumes, combined with an increase in larger mesopores and (possibly) macropores, as shown in the schematic presentation (Fig. 5) of the formation of the larger mesopores and macropores. Sample PEG351 also exhibited a macrophase separation, but in this case, there was no decrease in total pore volume.

An analysis of the specific external surface area of the samples will give an indication of the sample roughness. The only sample that differs from the others is sample PEG105, which displayed the Type IV adsorption isotherm, and did exhibit a macrophase separation during sol-gel processing. The remaining samples showing macrophase separation during sol-gel processing (PEG351 and PEG355) do not appear to exhibit higher specific external surface areas; their roughness may be due to the presence of macropores, which cannot be identified by nitrogen adsorption measurements.

Normally, a BET-derived specific surface area for a microporous solid has no physical meaning, however, such data may be used to make material comparisons (Gregg and Sing, 1982). The BET values were defined over the relative pressure range equivalent to the range (iii) in the α_S-plots; this method overcomes the problem of over-estimated BET values, due to enhancement of adsorption by the micropore field. This method generated results which agree very well with the specific SPE surface areas, summarised in Table 1. The agreement exceeds 10% for sample PEG355 since, no linear region exists in range (iii). A general trend of the results in Table 1 suggests the BET and specific SPE surface areas decrease with increasing PEG concentration. Comparing the effects of molecular weight on these data indicates that for a given molecular weight the data are almost constant valued. These results suggest that the pores are not formed as a consequence of the imbibed PEG because higher concentrations of PEG lead to a decrease in volume. We suggest the phase behaviour between the organic and inorganic polymers affects the porosity more than the burning and the sintering of the ceramic. These observations are consistent with those of Julbe et al. (1994) who found, using non-ionic surface-active agents which do not affect sol stability, that the increased molecular weight and concentration in the sol-gel mixture result in increased BET values for the microporous solids. We conclude the porosity in sol-gel derived ceramics may be controlled by a careful selection of an organic polymer which does not affect the sol-gel reaction stability.

Mesopore Size Distribution

Mesopore size distributions were determined using the method proposed by Barrett et al. (1951) applied to the desorption hysteresis branch of the isotherms. This method employs the Kelvin equation and a correction for adsorbed layer thinning during desorption from an assumed cylindrical pore model. The model calculates pores of radius $\geq$1.6 nm. Figure 6 shows typical results of these analyses. Clearly, each sample has pore radii $<$2.0 nm, except samples PEG105 and PEG355. Sample PEG0 has the smallest mean pore width, with a small but discernible increase in mean width with increasing PEG concentration. Sample PEG105 contains a wider pore size distribution when compared with the remaining samples with pores ranging from 6 nm to 20 nm and a small maximum at 3 nm (results not shown). Sample PEG355 exhibits slightly wider pores than the other samples in the PEG35x series, probably due to the effects of the macrophase separation encountered during the sol-gel formation (results not shown). The pores of sample PEG351 also originated from a macrophase separation but probably contains macropores, which are not detectable with nitrogen adsorption—mercury intrusion porosimetry would be necessary to define this pore size range.

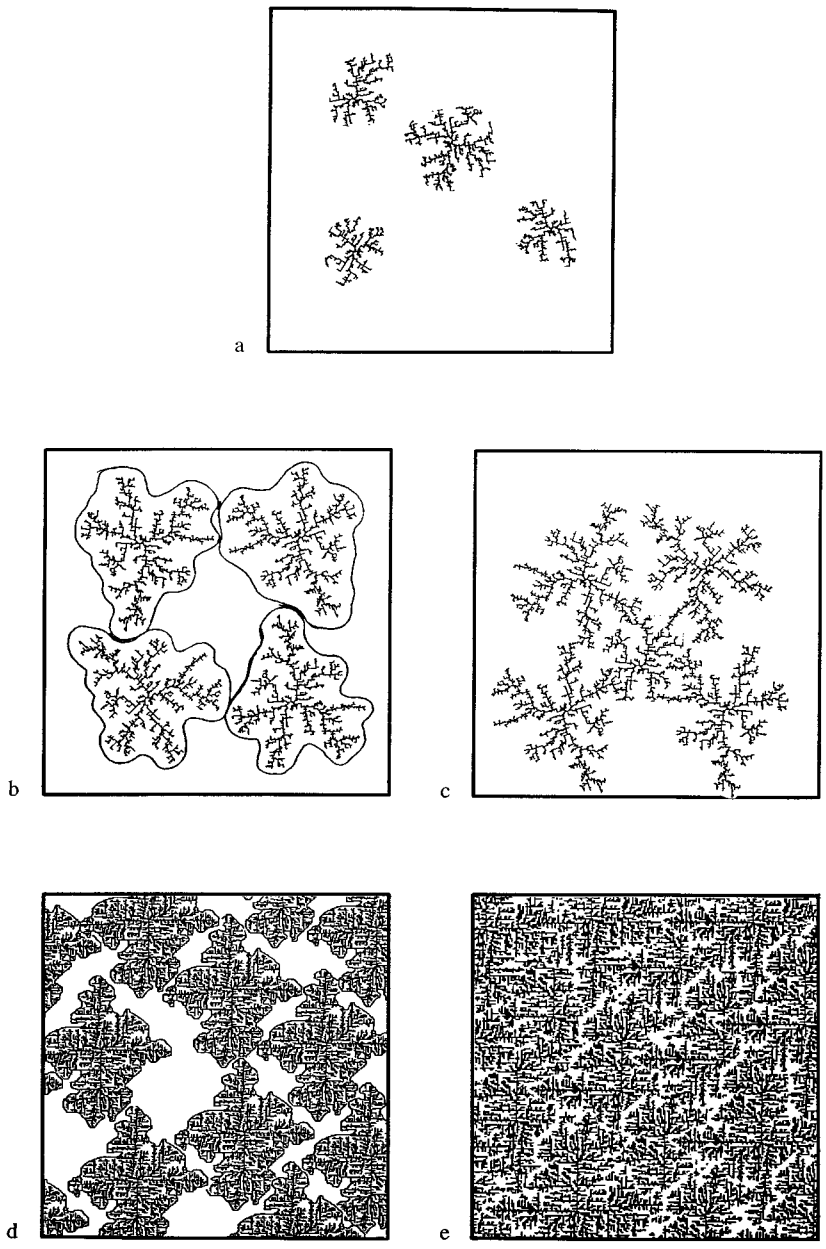

Figure 5. Schematic presentation of the formation of larger mesopores and macropores by phase separation by the incorporation of PEG in the sol. (a) TEOS sol with small inorganic clusters. (b) Sol with big inorganic clusters in the presence of PEG. (c) Sol with big inorganic clusters in the absence of PEG. (d) Ceramic material obtained from (b) burned at 973 K consisting of micropores, larger mesopores and/or macropores. (e) Ceramic material obtained from (c) burned at 973 K consisting of micropores.

Micropore Size Distribution

From shape factor analysis by thermoporosimetry Quinson et al. (1986) found that acid-catalysed silicas usually produce cylindrical pores. Consequently, the expected shape of the pores in our case is more likely a cylinder than a slit. Saito and Foley (1991) modified the slit-shaped model procedure for micropore width calculation proposed by Horvath and Kawazoe (1983). The cylinder model calculates an effective width or

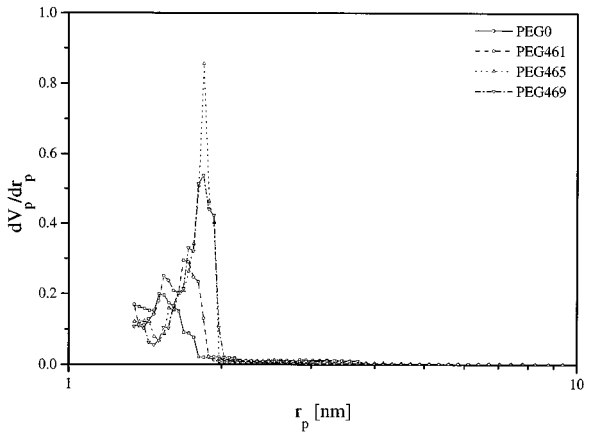

Figure 6. Pore size distribution curve by BJH method for samples PEG0, PEG461, PEG465 and PEG469.

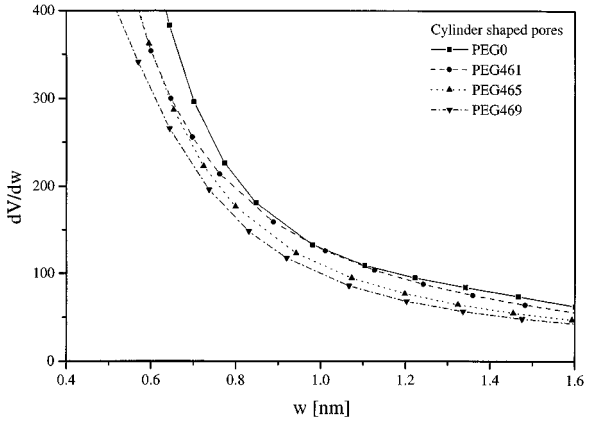

Figure 7. Micropore size distribution curve for samples PEG0, PEG461, PEG465 and PEG469 based on the cylinder shape pore model.

diameter of the pore and thus, as presented in Fig. 7, the micropores dimensions have been (correctly) adjusted to clarify the comparison with the calculated radius in the mesopore size distributions in Fig. 6. The micropore distributions for all of the samples prepared with the PEG template narrows in comparison with sample PEG0. Unfortunately, however, none of the distributions show a maximum. Two possible explanations may account for this fact: (1) the lower limit of pressure measurement in the equipment used to define the appropriate range of the isotherm is too high; (2) the pore size distribution in the micropore range is wide and no maximum is observed due to the lack of an inflection point in the adsorption data in the very low relative pressure region. From the procedures followed during the adsorption isotherm determination, this latter explanation is the more plausible. The pore size distribution curves narrow with increasing PEG concentration; PEG359 is the exception. These micropore distribution curves are consistent with the α_S-plot analyses. The condensation region (region (iv)) of the α_S-plots suggest a negligible secondary micropore content, equivalent to a radius $>3\sigma$, $\approx$1.0 nm.

Conclusions

A detailed analysis of the nitrogen adsorption-desorption isotherms have been made using several analytical techniques. The incorporation of a water-soluble polymer, of different molecular weight and/or concentration, in the sol-gel reaction mixture affects the eventual microstructural features of the ceramic producing materials containing micropores and mesopores. The phase behaviour, on a micro- and macroscale of the sol-gel process, also affect the structure of the eventual ceramic formed. Both the adsorption isotherms and the α_S-plot analyses indicate the presence of micropores in all of the ceramic materials produced. The α_S-plots contain a small filling swing associated with the presence of primary micropores. The addition of PEG to the sol-gel mixture affects the specific primary micropore volume, specific total pore volume, specific external surface area and the specific SPE surface area. The specific SPE surface area compares favourably with the specific BET surface area. Variations in the specific total pore volumes are assumed to originate from a macrophase separation which forms mesopores and macropores with a concomitant reduction in the total pore volume. Phase separation is also responsible for variations in the specific external surface area, a measure of the sample surface roughness. The good agreement between the specific BET and SPE surface areas indicate that the phase behaviour between the organic and inorganic polymers are more porosity-determining than the "holes" caused by burning, and removing, the imbibed PEG template. The presence of PEG in the sol-gel mixture results in an increase in the most frequent width in the mesopore size distribution, determined using the BJH method of analysis. The macrophase separation in PEG105 caused considerable widening of the mesopore size distribution. The micropore size distribution, also calculated assuming a cylindrical-pore shape, was somewhat inconclusive due to the lack of a maximum in the effective width distribution. The overall analysis of the distributions

were consistent with the α_S-plot analyses, very small pores in the primary micropore range predominate with a nominal contribution from the secondary micropore volume.

Acknowledgements

The authors wish to thank Prof. K.S.W. Sing for fruitful discussions about the α_S plots. Further, the Academy of Finland and the Ministry of Education (Finland) are gratefully acknowledged for financial support.

References

Ågren, P. and J.B. Rosenholm, "Phase Behaviour and Structural Changes in Tetraethylorthosilicate Derived Gels in Presence of Polyethylene Glycol—studied by Rheological Techniques and Visual Observations," *J. Colloid Interface Sci.*, **204**, 45 (1998).

Barrett, E.P., L.G. Joyner, and P.P. Halenda, "The Determination of Pore Volume and Area Distributions in Porous Substances. I. Computations from Nitrogen Isotherms," *J. Am. Chem. Soc.*, **73**, 373 (1951).

Beck, J.S., J.C. Vartuli, W.J. Roth, M.E. Leonowicz, C.T. Kresge, K.D. Schmitt, C.T.-W. Chu, D.H. Olson, E.W. Sheppard, S.B. McCullen, J.B. Higgins, and J.L. Schlenker, "A New Family of Mesoporous Molecular Sieves Prepared with Liquid Crystal Templates," *J. Am. Chem. Soc.*, **114**, 10834 (1992).

Bhambhani, M.R., P.A. Cutting, K.S.W. Sing, and D.H. Turk, "Analysis of Nitrogen Isotherms on Porous and Nonporous Silicas by the BET and α_S Methods," *J. Colloid Interface Sci.*, **38**, 109 (1972).

Brinker, C.J. and G.W. Scherer, *Sol-Gel Science*, Academic Press, San Diego, 1990.

Gregg, S.J. and K.S.W. Sing, *Adsorption, Surface Area and Porosity*, Academic Press, London, 1982.

Hanzawa, Y., K. Kaneko, R.W. Pekala, and M.S. Dresselhaus, "Activated Carbon Aerogels," *Langmuir*, **12**, 6167 (1996).

Horvath, G. and K. Kawazoe, "Method for the Calculation of Effective Pore Size Distribution in Molecular Sieve Carbon," *J. Chem. Eng. Japan*, **16**, 470 (1983).

Julbe, A., C. Balzer, J.M. Barthez, C. Guizard, A. Larbot, and L. Cot, "Effect of Non-Ionic Surface Active Agents on TEOS-Derived Sols, Gels and Materials," *J. Sol-Gel Sci. Technol.*, **4** (1994).

Kaneko, K., "Determination of Pore Size and Pore Size Distribution 1. Adsorbents and Catalysts," *Journal of Membrane Science*, **96**, 59 (1994).

Kaneko, K. and C. Ishii, "Superhigh Surface Area Determination of Microporous Solids," *Colloid Surf.*, **67**, 203 (1992).

Kaneko, K., C. Ishii, M. Ruike, and H. Kuwabara, "Origin of Superhigh Surface Area and Microcrystalline Graphitic Structures of Activated Carbons," *Carbon*, **30**, 1075 (1992).

Kunze, K. and D. Segal, "Modification of the Pore Structure of Sol-Gel-derived Ceramic Oxide Powders by Water-Soluble additives," *Colloids and Surf.*, **58**, 327 (1991).

Matsuoka, H., S. Chen, H. Ishii, N. Ise, K. Nakanishi, and N. Soga, "Small-Angle X-ray Scattering Study on Sol-Gel Transition of mixtures of colloidal Silica and Organic Polymer," *Bull. Chem. Soc. Jpn.*, **64**, 1283 (1991).

Nakanishi, K., H. Komura, R. Takahashi, and N. Soga, "Phase Separation in Silica Sol-Gel System Containing Poly(ethylene oxide). I. Phase Relation and Gel Morphology," *Bull. Chem. Soc. Jpn.*, **67**, 1327 (1994).

Nakanishi, K., R. Takahashi, and N. Soga, "Dual-Porosity Silica Gels by Polymer-Incorporated Sol-Gel Process," *J. Non-Cryst. Sol.*, **147/148**, 291 (1992).

Quinson, J.F., J. Dumas, and J. Surughetti, "Alkoxide Silica Gel: Porous Structure by Thermoporosimetry," *J. Non-Cryst. Sol.*, **79**, 397 (1986).

Saito, A. and C. Foley, "Curvature and Parametric Sensitivity in Models for Adsorption in Micropores," *AIChE J.*, **37**, 429 (1991).